International Journal of Nanomedicine

Dovepress
open access to scientific and medical research

Open Access Full Text Article

ORIGINAL RESEARCH

Ultra-small gadolinium oxide nanocrystal sensitization of non-small-cell lung cancer cells toward X-ray irradiation by promoting cytostatic autophagy

This article was published in the following Dove Medical Press journal:
International Journal of Nanomedicine

Feifei Li[1,2,*]
Zihou Li[2,3,*]
Xiaodong Jin[1]
Yan Liu[1]
Pengcheng Zhang[1,2]
Ping Li[1]
Zheyu Shen[3]
Aiguo Wu[3]
Weiqiang Chen[1]
Qiang Li[1]

[1]Institute of Modern Physics, Chinese Academy of Sciences, Key Laboratory of Heavy Ion Radiation Biology and Medicine of Chinese Academy of Sciences, Key Laboratory of Basic Research on Heavy Ion Radiation Application in Medicine, Gansu Province, Lanzhou 730000, China; [2]University of Chinese Academy of Sciences, Beijing 100049, China; [3]Key Laboratory of Magnetic Materials and Devices, Chinese Academy of Sciences, Division of Functional Materials and Nano Devices, Ningbo Institute of Materials Technology and Engineering, Chinese Academy of Sciences, Ningbo, Zhejiang 315201, China

*These authors contributed equally to this work

Correspondence: Weiqiang Chen; Qiang Li
Institute of Modern Physics, Chinese Academy of Sciences, 509 Nanchang Road, Lanzhou 730000, China
Tel +86 931 496 9316
Email chenwq7315@impcas.ac.cn; liqiang@impcas.ac.cn

Background: Gadolinium-based nanoparticles (GdNPs) have been used as theranostic sensitizers in clinical radiotherapy studies; however, the biomechanisms underlying the radiosensitizing effects of GdNPs have yet to be determined. In this study, ultra-small gadolinium oxide nanocrystals (GONs) were employed to investigate their radiosensitizing effects and biological mechanisms in non-small-cell lung cancer (NSCLC) cells under X-ray irradiation.

Method and materials: GONs were synthesized using polyol method. Hydroxyl radical production, oxidative stress, and clonogenic survival after X-ray irradiation were used to evaluate the radiosensitizing effects of GONs. DNA double-strand breakage, cell cycle phase, and apoptosis and autophagy incidences were investigated in vitro to determine the radiosensitizing biomechanism of GONs under X-ray irradiation.

Results: GONs induced hydroxyl radical production and oxidative stress in a dose- and concentration-dependent manner in NSCLC cells after X-ray irradiation. The sensitizer enhancement ratios of GONs ranged between 19.3% and 26.3% for the NSCLC cells under investigation with a 10% survival rate compared with that of the cells treated with irradiation alone. Addition of 3-methyladenine to the cell medium decreased the incidence rate of autophagy and increased cell survival, supporting the idea that the GONs promoted cytostatic autophagy in NSCLC cells under X-ray irradiation.

Conclusion: This study examined the biological mechanisms underlying the radiosensitizing effects of GONs on NSCLC cells and presented the first evidence for the radiosensitizing effects of GONs via activation of cytostatic autophagy pathway following X-ray irradiation.

Keywords: gadolinium oxide nanocrystal, radiosensitization, cytostatic autophagy, apoptosis, oxidative stress

Introduction

Cancer, the second leading cause of mortality, is responsible for 9.6 million deaths globally. Approximately 18.4% of total cancer deaths can be attributed to lung cancer, which resulted in 1.76 million deaths in 2018.[1] Radiotherapy, as well as surgery and chemotherapy, is one of the standard treatments for advanced lung cancer as indicated in multiple guidelines.[2,3] The combination of radio- and chemotherapy results in significant improvements in local tumor control and cure rates. Among these combined treatments, the combination of platinum-based chemotherapy with intensity-modulated radiotherapy is an effective method for non-small-cell lung cancer (NSCLC) therapy.[4] However, the five-year survival rate for NSCLC, the most common type of lung cancer,

submit your manuscript | www.dovepress.com
Dovepress
http://dx.doi.org/10.2147/IJN.S193676

is only 16.1%.[5] Elevated radiation doses during radiotherapy may improve the local control of resistant tumors located in the lung, but it increases the risk of side effects in the lungs and heart.[6] A safer and more effective methodology, which can either elevate the radiation dose to the tumor or improve the damage to the tumor while sparing the organs at risk, is needed for advanced NSCLC treatment.

Nanomaterials, which can accumulate in tumors either by enhanced permeability and retention effect or by the use of targeting biomolecules,[7] have been developed as nano-enhancers to improve the biological effects of physical irradiation dose. High-Z metal-based nanoparticles possess high X-ray photon capture cross-sections and are capable of increasing the production of secondary and Auger electrons, which in turn increases the generated reactive oxygen species (ROS) and enhances radiotherapy.[8,9] In addition to gold nanoparticles, which are the first and most studied nanoparticles and the enhancement effects of which have been demonstrated both in vitro and in vivo,[10–12] gadolinium-based nanoparticles (GdNPs) have also attracted substantial attention because of their high relaxation time and high atomic number (Z=64).[13–16] Ultra-small gadolinium oxide nanocrystals (GONs) are attractive GdNPs that possess a high density of Gd per contrast-agent unit (200–400 atoms per particle).[17] GONs have been developed as advanced T_1-weighted MRI contrast agents due to their high longitudinal relaxivities and small r_2/r_1 ratios.[18–20] The radiosensitization properties of GONs were first investigated by Amirrashedi et al in a gel-filled phantom, in which the maximum dose enhancement of GONs ranged from 15% to 24%.[21] Seo et al found that the GONs enhancement of the production of ROS under photon and proton irradiation was dose-dependent with a factor of 1.94 compared with that of the radiation-only control. Core-inner-valence ionization of GONs can de-excite electrons via potent Gd-Gd interatomic de-excitation processes.[22] Previous studies have revealed the physical or chemical mechanisms of the dose enhancement effects of GONs, but no biological mechanism for GONs has been determined yet. The radiosensitizing biomechanism of GONs under X-ray irradiation remains unclear.

Our work has focused on the biological mechanisms of ionizing radiation, including the radiosensitizing mechanisms of nanoparticles.[23–25] The aim of the present study was to evaluate the radiosensitizing effects and mechanism of GONs in NSCLC cells under X-ray irradiation. After the cellular uptake and cell viability of GONs in NSCLC cells were studied, the clonogenic survival fractions of human NSCLC cells were investigated in the presence of GONs under X-ray irradiation compared to that of cells treated with irradiation alone. Then, the enhancements of hydroxyl radical production and oxidative stress under X-ray irradiation in the presence of GONs were confirmed. Further studies on autophagy and apoptosis levels as well as DNA damage unraveled the biological mechanism of GONs sensitization to X-ray irradiation in NSCLC cells.

Methods

Synthesis of GONs

GONs were synthesized following a previously reported method.[26] Briefly, 26 mL of a 0.1 g/mL solution of gadolinium(III) nitrate hexahydrate ($Gd(NO_3)_3{\cdot}6H_2O$, 99%) in diethylene glycol (DEG, 99%) was heated to 100°C with vigorous stirring. Afterward, 34 mg of sodium hydroxide (NaOH, 99%) in 34 mL DEG was slowly added dropwise into the $Gd(NO_3)_3{\cdot}6H_2O$ solution. After refluxing for 60 minutes at 140°C, the temperature of the mixture was raised to 175°C for another 4 hours. The obtained GONs sample was naturally cooled and purified by membrane dialysis with a cut-off of 3,500 Da for 72 hours with Milli-Q water. The water was replaced with fresh water every 8 hours. The reagent chemicals were all purchased from Aladdin Industrial Inc. (Shanghai, China).

High-resolution transmission electron microscopy

The dilute GONs dispersion (1.0 µL) was added dropwise onto a copper grid coated with a thin layer of carbon film and then dried at room temperature. High-resolution transmission electron microscopy (HRTEM) images were recorded on a JEOL-2100 (JEOL, Tokyo, Japan) instrument operated at 200 kV.

Dynamic light scattering (DLS) measurement

The hydrodynamic diameter of the GONs was measured at room temperature by DLS using a zeta particle size analyzer (Nano-ZS, Malvern, England). The data were collected on an autocorrelator with a detection angle for the scattered light of 173°.

UV-Vis spectra measurement

Solutions of GONs (200 µL) with various concentrations and incubation times in the medium were added into the wells of 96-well plates. Then, the absorption spectra of the GONs were obtained using a UV-Vis spectrophotometer (Jasco, Tokyo, Japan) by scanning from 200 to 900 nm with a resolution of 2.0 nm.

Cell culture

Human NSCLC cell lines (A549, NH1299, and NH1650) were purchased from the Type Culture Collection of the Chinese Academy of Sciences (Shanghai, China) and grown in RPMI 1640 Medium (Thermo Fisher Scientific Inc., Waltham, MA, USA) containing 10% heat-inactivated fetal bovine serum (Bailing Bio, Lanzhou, China) at 37°C in a humidified 5% CO_2 atmosphere. In the autophagic study, cells were pretreated with 3-methyladenine (3-MA), an inhibitor of autophagy, for 4 hours before irradiation.

Gd concentration analysis

The Gd concentration was measured by inductively coupled plasma atomic emission spectrometry on an IRIS ER/S (Thermo Jarrell Ash, USA) using an external calibration method.[19] To obtain cellular Gd concentrations, the cells were pretreated with various concentrations (0.5, 1.0, 5.0, 10.0, and 20.0 μg/mL) of Gd for 24 hours. The cells were harvested, counted, and dried, and then resuspended and ionized in 1.0 mL of aqua regia. After measurement, the cellular Gd mass was calculated by dividing the Gd content by the total cell number.

Cell viability

To detect the viability of cells pretreated with GONs, a CCK-8 kit was used for sensitive colorimetric assays for the determination of proliferation and cytotoxicity. Initially, approximately 10,000 cells per well were plated into 96-well plates and cultured overnight to adhere. Then, the cells were co-incubated with multiple concentrations (0, 0.2, 0.5, 1, 5, 10, 20, and 50 μg/mL) of Gd for 24 hours. Afterwards, the cells were washed twice with PBS, incubated in medium containing CCK-8 while protected from light, and then detected at a wavelength of 450 nm by a microplate reader (Thermo Fisher Scientific Inc.) within 4 hours. The absorbances were normalized to the signal intensity of cells without GONs treatment.

Measurement of hydroxyl radical production

A solution of 3-coumarin carboxylic acid (3-CCA; J&K Chemical Co. Ltd, China) was prepared according to a previously reported method.[27] Then, dilute solutions, of which the Gd concentrations were 0, 0.5 and 5.0 μg/mL with or without radiation treatment were equally divided among the wells of black 96-well culture plates and measured at an excitation wavelength of 395 nm and emission wavelength of 442 nm with a microplate reader (Infinite F200/M200, TECAN Co., Switzerland).

Detection of ROS

ROS were evaluated using 2,7-dichlorohydrofluoroscein diacetate (DCFH-DA; Solarbio Life Sciences, China) as a probe. DCFH-DA was co-incubated with irradiated cells with or without the preincubation of GONs in serum-free medium for 30 minutes at 37°C. Then, the fluorescent signals of the cells in a 96-well plate were detected at 525 nm with an excitation wavelength of 488 nm using a microplate reader (Thermo Fisher Scientific Inc.). Afterwards, the mean cellular fluorescence was calculated by dividing the fluorescent signals by the total number of counted cells.

Irradiation

Cells were plated into T25 flasks or 35-mm petri dishes 24 hours before incubation with GONs, and the concentrations of Gd in the medium were 0.5 and 5.0 μg/mL. X-ray irradiation was performed with an X-ray machine (PXi, North Branford, CT, USA) operating at 225 kV at room temperature. The dose rate was 2.0 Gy/min.

Flow cytometry

Cells were preincubated with GONs for 24 hours in 35-mm petri dishes and then irradiated by 2.0 Gy X-ray. The rate of apoptosis was detected according to the protocol provided by the manufacturer using an Annexin V–FITC and propidium iodide (PI) apoptosis kit (Roche Diagnostics, Indianapolis, IN, USA). To measure autophagy incidence, cells were incubated with a 1.0 μg/mL solution of acridine orange for 15 minutes, washed, collected, and then quantified by flow cytometry (Sysmex CyFlow Cube 6) at the indicated postirradiation times. The influences of GONs and/or radiation treatments on cell cycle progression were analyzed with flow cytometry. After being harvested and fixed in 70% ice-cold ethanol at –20°C for 48 hours, the cells were stained for 20 minutes on ice with PBS containing 100 μg/mL RNase, 0.2% Triton X-100, and 50 μg/mL PI (Sigma-Aldrich Co., St Louis, MO, USA).

Western blot analysis

Total cellular extracts were prepared as previously described[28] and transferred to polyvinylidine difluoride membranes. Blots were visualized by enhanced chemiluminescence after incubation with the indicated antibodies. The primary antibodies used in this study included GAPDH, LC3, caspase-3, Bcl-2,

Bax, Bip, Drp1, and p-Drp1 (all acquired from Cell Signaling Technology, Danvers, MA, USA).

Clonogenic survival assay

Cells with different treatments were suspended after X-ray irradiation with 0, 1.0, 2.0, 3.0, and 4.0 Gy. The cell suspensions were then counted, diluted, and finally seeded into Φ60 petri dishes with 5 mL of complete media. After 14 days of incubation, the colonies were stained with crystal violet for 30 minutes and carefully washed. Colonies with more than 50 cells were recorded as survivors and counted manually under an inverted microscope. Measured survival data were fit using the linear-quadratic (LQ) model.

Immunofluorescence assay

NSCLC cells were pretreated with GONs for 24 hours, followed by exposure to 2.0 Gy X-rays. Then, at 1, 4, and 12 hours post-irradiation, the cells were fixed using 4% paraformaldehyde, permeabilized with 0.3% Triton X-100, and subsequently blocked with 5% BSA at room temperature for 1 hour. After incubation with a primary monoclonal antibody against γ-H2AX at 4°C overnight, the cells were washed and incubated with a donkey anti-rabbit IgG-FITC secondary antibody for 1.5 hour at room temperature. The nuclei of the cells were then stained with Hoechst stain for 10 minutes. Finally, the foci were observed with a confocal microscope (Leica, Wetzlar, Germany). Mean fluorescent values of the foci were determined by at least 50 cells.

Statistical analysis

Quantitative data are expressed as mean ± SD. Comparisons of the data derived from the control and treatment samples were performed using one-way ANOVA with SPSS v. 16.0 software (SPSS/IBM Corp., Armonk, NY, USA). Differences were considered statistically significant and statistically extremely significant when $p<0.05$ and $p<0.01$, respectively.

Results

Characteristics of GONs

Ultra-small GONs were synthesized and dialyzed and their average core size was approximately 3.1 nm, as revealed by HRTEM (Figure 1A, core diameter calculated from more than 100 nanoparticles). As shown in the inset of Figure 1A, the HRTEM images of the particles indicate a regular crystalline lattice with (222) planes (d ≈ 3.1 Å). This is consistent with the literature results.[19,26] The hydrodynamic diameter of GONs is 8.71±2.78 nm (Figure 1B); this increase in size is due to the formed hydration corona. We measured the zeta potential of the GONs (52.6 mV). A dispersed solution of the synthesized GONs, the Gd concentration of which is 15.52 mg/mL according to ICP-AES analysis, is clear brown in color and can be stored at 4°C for several months without aggregation. The GONs are stable in RPMI 1640 medium (Figure S1).

Cellular toxicity and uptake of GONs in NSCLC cells

We investigated the cytotoxicity of GONs in three NSCLC cell lines (A549, NH1299, and NH1650). As shown in Figure 2A, the cell viabilities of the three studied cell lines incubated with GONs increased slightly with increasing GONs concentration over which the Gd concentrations are 0, 0.2, 0.5, 1, 5, 10, 20, 50 μg/mL. These results demonstrate that GONs exhibited good biocompatibility without obvious cytotoxicity. Then, we investigated the Gd content in A549, NH1299, and NH1650 cells as shown in Figure 2B. Based on the ICP-AES measurement, the mass of intracellular Gd in NH1299 cells was approximately 1.24 pg/cell, which was much higher than the 0.51 pg/cell in A549 cells and 0.082 pg/cell in NH1650 cells, at an incubated Gd concentration of 0.5 μg/mL. The intracellular mass of Gd in NH1299 cells increased much faster with increasing incubation concentration than those in A549 and NH1650 cells. Because large differences existed in the cytotic mass of Gd in the three studied cell lines, we used the same coculture concentrations for the following studies.

Effects of GONs pretreatment on cellular sensitivity to X-ray irradiation

We investigated the survival fractions of the three studied NSCLC cell lines under X-ray irradiation in the absence or presence of GONs, for which the Gd concentrations used in the culture were 0.5 and 5.0 μg/mL. The survival data in each case were fit with LQ model.[23] The clonogenic survival curves are presented in Figure 3A–C. Compared with X-ray irradiation alone, co-treatment (X-ray irradiation and GONs) caused a more abrupt decrease in the survival curves of the A549 and NH1299 cells at a Gd concentration of 0.5 μg/mL, but no obvious decrease in that of the NH1650 cells was observed; when the co-cultivated GONs were increased to a 5.0 μg/mL Gd concentration, stronger decreases were observed in the survival curve of the NH1650 cells compared to that of irradiation alone.

Using a reported method,[23] the sensitizer enhancement ratio (SER) was calculated. As shown in Table 1, the SERs at the 10% cell survival fraction level (SF_{10}) of 0.5 μg/mL

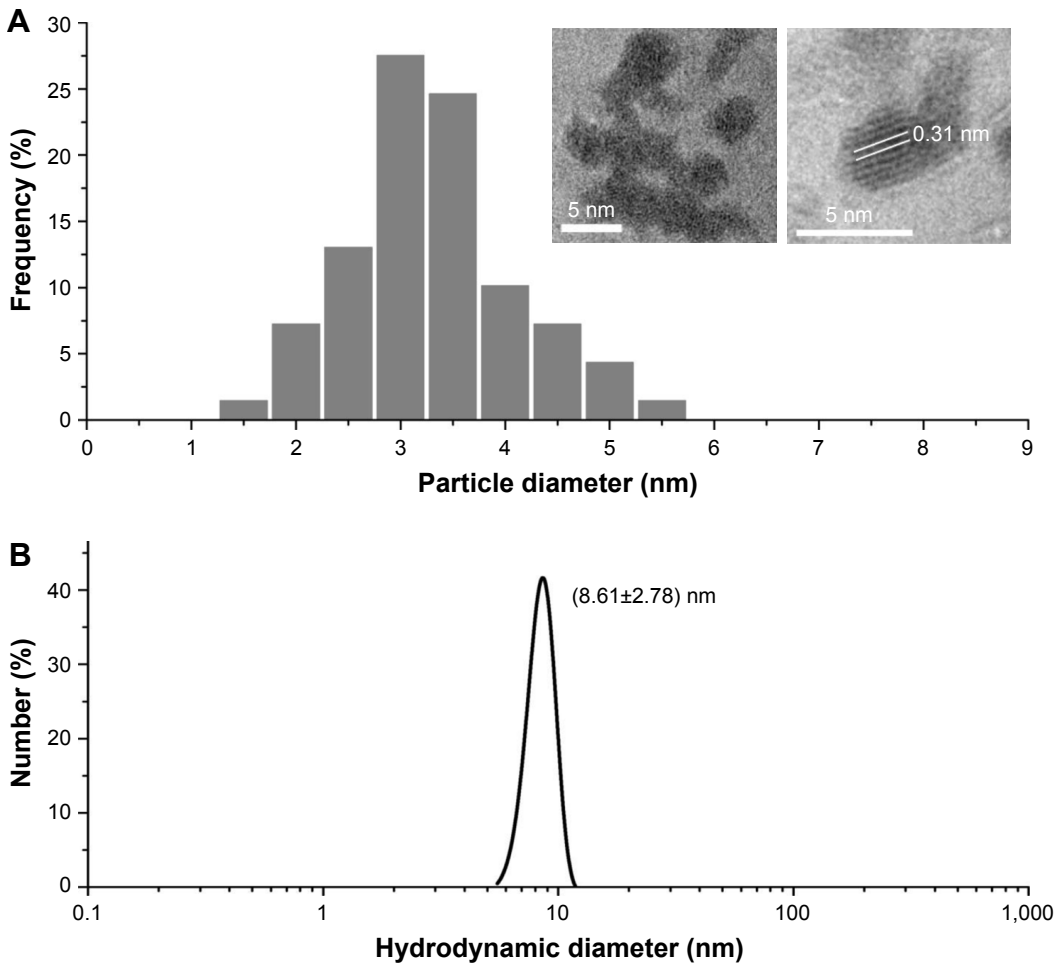

Figure 1 Diameter of GONs.
Notes: (**A**) Size distribution of nanoparticles as visualized by high-resolution transmission electronic microscopy and (**B**) dynamic light scattering profiles of GONs suspensions.
Abbreviation: GONs, gadolinium oxide nanocrystals.

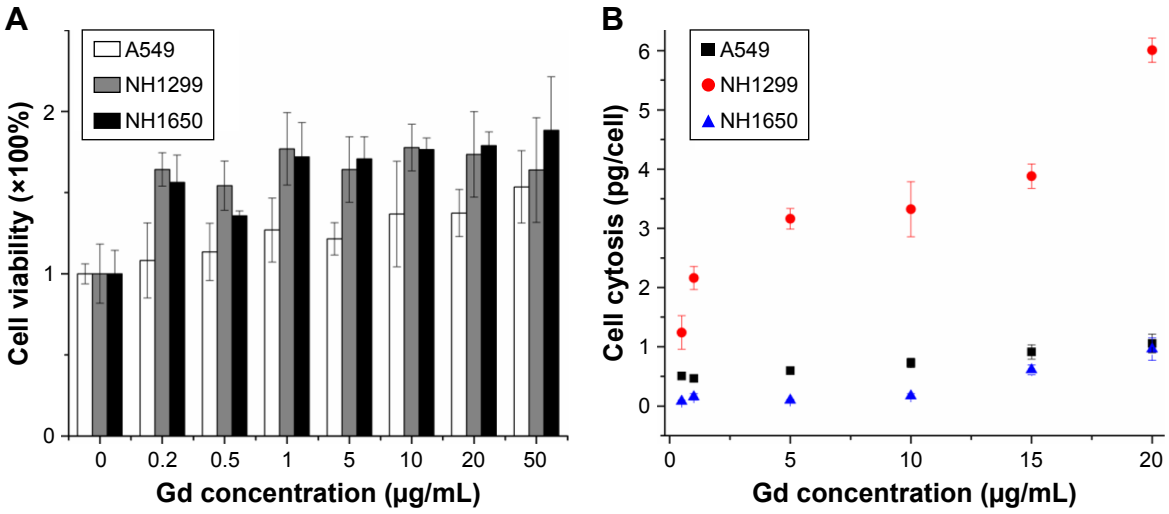

Figure 2 Cytotoxicity and cellular uptake of GONs in NSCLC cells.
Notes: (**A**) Cytotoxicity of GONs at an incubation time of 24 hours using a CCK-8 kit. (**B**) Relationship between cellular uptake of Gd in the three studied cell lines and the incubated Gd concentration.
Abbreviations: GONs, gadolinium oxide nanocrystals; NSCLC, non-small-cell lung cancer; Gd, gadolinium.

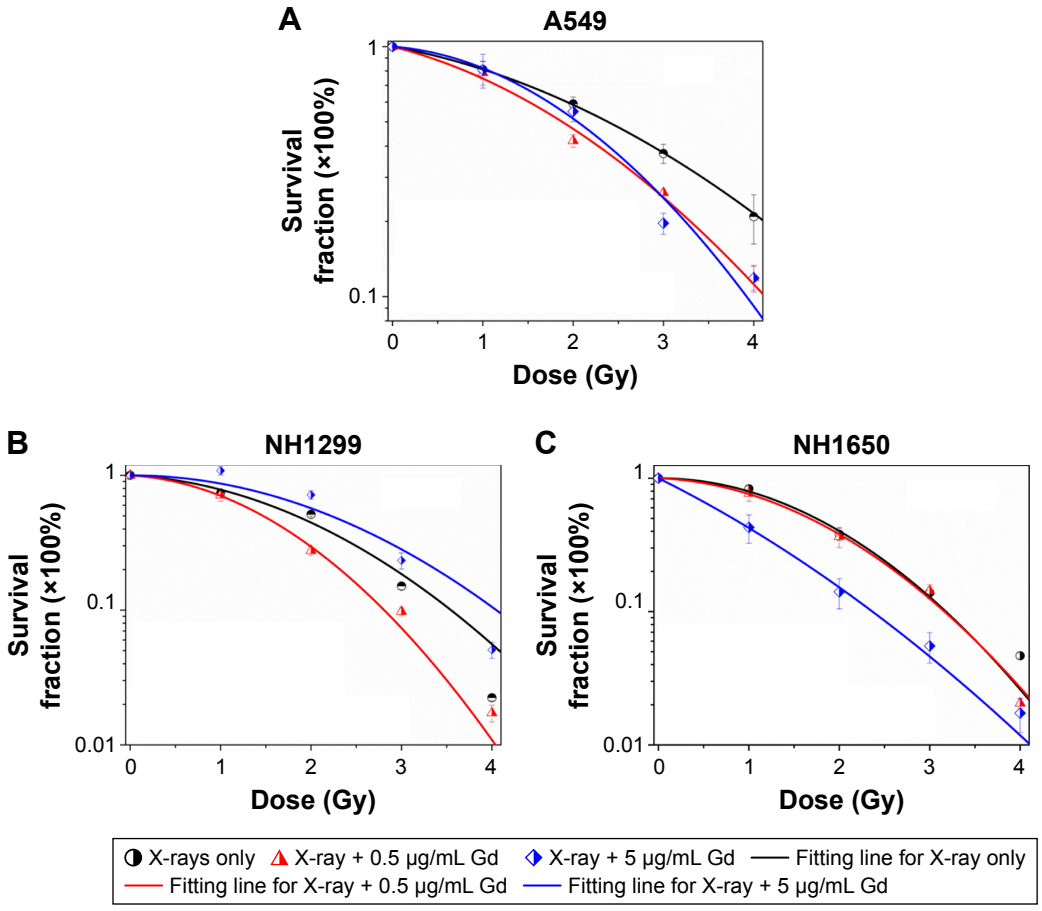

Figure 3 Effects of pretreatment with GONs on the cellular sensitivity to X-ray irradiation.
Notes: Clonogenic assay of A549 (**A**), NH1299 (**B**), and NH1650 (**C**) cells exposed to radiation.
Abbreviation: GONs, gadolinium oxide nanocrystals.

of Gd were 19.3%, 20.6%, and 1.6% in A549, NH1299, and NH1650 cells, respectively. The addition of 5.0 μg/mL Gd led to a stronger radiosensitizing effect on the NH1650 cells with an SER_{SF10} of 26.3% and SER_{SF50} of 53.4%. These results indicate that GONs can enhance the radiation sensitivity of the three studied NSCLC cell lines to X-ray irradiation in a concentration-dependent manner. The large differences in the radiation enhancements of the GONs found in this study may relate to the Gd concentrations in the three studied NSCLC cell lines.

Table 1 Summary of fitting parameters, D_{SF}, and SER_{SF} in the absence and presence of GONs

X-ray irradiation	α (Gy^{-1})	β (Gy^{-2})	R^2	D_{SF10} (Gy)	SER_{SF10}	D_{SF50} (Gy)	SER_{SF50}
A549 control	0.152	0.058	0.999	5.12		2.40	
0.5 μg/mL Gd	0.210	0.0842	0.989	4.13	19.3%	1.88	21.7%
5.0 μg/mL Gd	0.066	0.133	0.986	3.92	23.4%	2.04	15.0%
NH1299 control	0.085	0.159	0.987	3.54		1.84	
0.5 μg/mL Gd	0.089	0.260	0.998	2.81	20.6%	1.46	20.7%
5.0 μg/mL Gd	0.009	0.140	0.921	4.06	−14.7%	2.21	−20.1%
NH1650 control	0.062	0.225	0.996	3.20		1.75	
0.5 μg/mL Gd	0.063	0.210	0.999	3.15	1.6%	1.66	5.1%
5.0 μg/mL Gd	0.774	0.0844	0.999	2.36	26.3%	0.815	53.4%

Notes: Coefficients α, β, and R^2 are the fitting parameters using a linear-quadratic model; D_{SF10} and D_{SF50} represent X-ray irradiation dose at 10% or 50% cell survival fraction, respectively; SER_{SF10} or SER_{SF50} represents sensitizer enhancement ratios of the irradiated NSCLC cells at 10% or 50% cell survival fraction.
Abbreviations: SFR, survival fraction level; NSCLC, non-small-cell lung cancer; Gd, gadolinium.

GONs result in hydroxyl radical and oxidative stress production after X-ray irradiation

Ionizing radiation results in the radiolysis of water and contributes to hydroxyl radical production. We examined the radiation enhancement ratio of the GONs on hydroxyl radical production in aqueous solutions exposed to X-rays using 3-CCA as a probe following the reported procedure.[23] The fluorescence intensities of the irradiated solutions were linearly dependent on the irradiation doses (Figure 4A). The dependence of the radiation enhancement ratios of the GONs on the radiation dose is shown in Figure 4B. The dose enhancement ratios for GONs are 1.44 and 1.22 at 0.5 Gy and 1.18 and 1.28 at 2.0 Gy, when the Gd concentrations in solution are 0.5 and 5.0 μg/mL, respectively. The dose enhancement ratios are in good agreement with the results of a previous study.[21] These results demonstrate that the presence of GONs increases hydroxyl radical production; moreover, the radiation enhancement effects of GONs on hydroxyl radical production in aqueous solutions induced by X-rays are dependent on dose and concentration.

Studies have shown that oxidative stress produced by nanomaterials can be observed in multiple cell types.[29] The ROS can be visualized to determine the oxidative stress levels in cells with or without GONs pretreatment after X-ray irradiation using DCFH-DA as a fluorometric probe.[30] The normalized fluorescence intensities of the studied cells are shown in Figure 4C–E. The oxidative stress levels induced by 2.0 Gy X-ray irradiation alone were 1.16-, 1.58-, and 1.33-fold higher than that of the controls for A549, NH1299, and NH1650 cells, respectively. When cocultured with GONs, at a Gd concentration of 0.5 μg/mL for A549 and NH1299 cells and 5.0 μg/mL for NH1650 cells, the oxidative stress levels increased to be 1.39-, 2.01-, and 1.92-fold higher than that of the controls for A549, NH1299 and NH1650 cells after X-ray irradiation, respectively. These results indicate that the addition of GONs contributes to 19.8%, 27.2%, and 44.4% of the oxidative stress enhancement in A549, NH1299, and NH1650 cells, respectively, which is in agreement with the results of the clonogenic survival assay.

Presence of GONs did not increase DNA damage after X-ray irradiation

Generally, radiation-induced nuclear DNA damage, such as single- and double-strand breakages (DSB), if left unrepaired, has been regarded as the main cause of mutation and

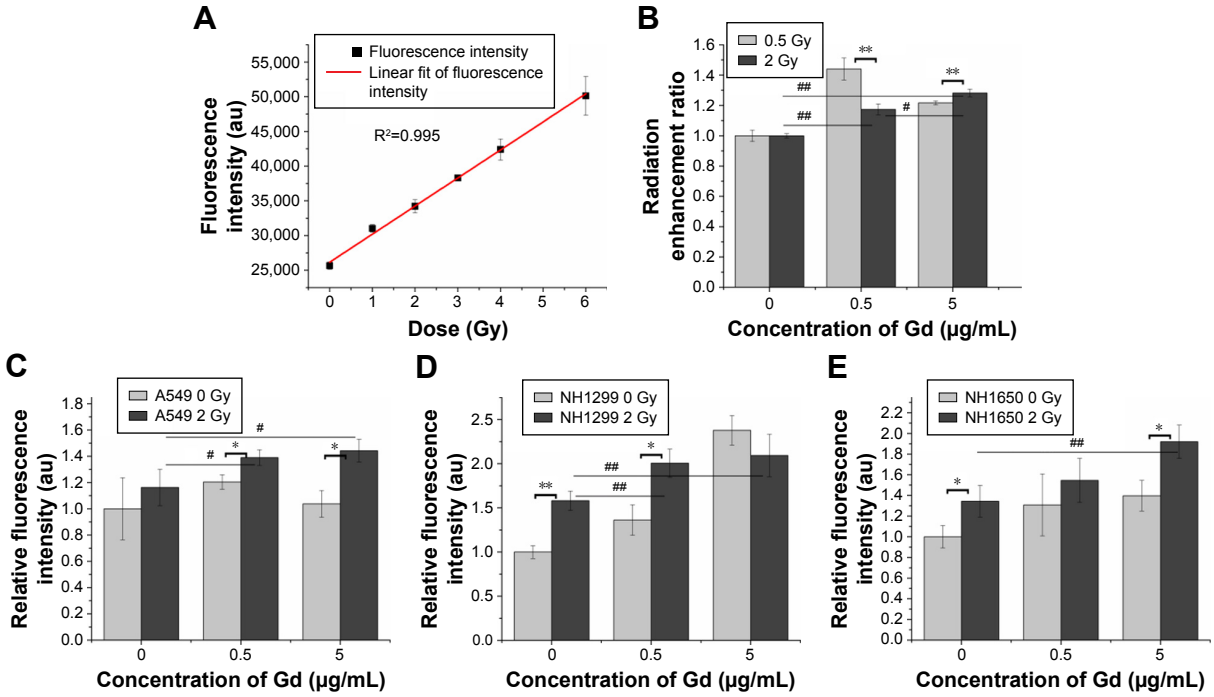

Figure 4 GONs cause hydroxyl radical and oxidative stress production after their uptake by irradiated NSCLC cells.
Notes: (**A**) Dependence of the fluorescence intensity variations of 3-CCA on the X-ray irradiated dose without GONs. (**B**) Hydroxyl radical enhancement of GONs. Oxidative stress levels as detected by DCFH-DA in A549 (**C**), NH1299 (**D**), and NH1650 (**E**) cell lines pretreated with GONs. *$p<0.05$ or **$p<0.01$ represents statistically significant or extremely significant differences induced by various radiation dosages. Similarly, #$p<0.05$ or ##$p<0.01$ indicates significant differences caused by different Gd concentrations.
Abbreviations: DCFH-DA, 2,7-dichlorohydrofluoroscein diacetate; GONs, gadolinium oxide nanocrystals; NSCLC, non-small-cell lung cancer.

cell death.[31] As one of the key events in the DNA damage response, γ-H2AX on Ser139 is considered to be a marker for DSB.[32] We investigated γ-H2AX foci in the studied NSCLC cells to assess the influence of GONs pretreatment on DNA DSBs induced by X-ray irradiation. As shown in Figure 5, no obvious difference was observed in foci formation between the combined treatment and X-ray irradiation alone, which indicates that cell lethality may derive from damage to the cytoplasm.

Defending the integrity of the genome is the purpose of the DNA damage response, and cell cycle checkpoints are activated, which are thought to allow cells to have time to repair their damaged DNA before moving to the next stage of the cell cycle. The cell cycles of the three studied cell lines under X-ray irradiation with or without GONs were analyzed (Figure S2). Irradiation (2.0 Gy) induced obvious G2/M phase arrest in the three NSCLC cell lines, whereas co-treatment did not notably enhance the cell phase arrest, which suggests that no additional DNA damage is produced though pretreatment of the cells with GONs. Consequently, the target of GONs radiosensitization of NSCLC cells to X-ray irradiation may be located in the cytoplasm but not in the nucleus.

GONs enhance apoptosis in A549 and NH1650 cells but not in NH1299 cells after X-ray irradiation

Cell apoptosis was measured in A549 as well as in NH1299 and NH1650 cells after various treatments using an Annexin V–FITC and PI apoptosis kit (Figures 6A and S3). As shown in Figure 6B, compared to the control, treatment with GONs alone had a slight influence on the apoptotic levels of the A549 cells, whereas 2.0 Gy of X-ray irradiation caused a gradual and moderate increase in the apoptotic levels, which is an enhancement compared with that of cells pretreated with GONs. Similar results were observed in NH1650 cells; however, the apoptosis levels of the p53-negative NH1299 cells never changed even after different treatment

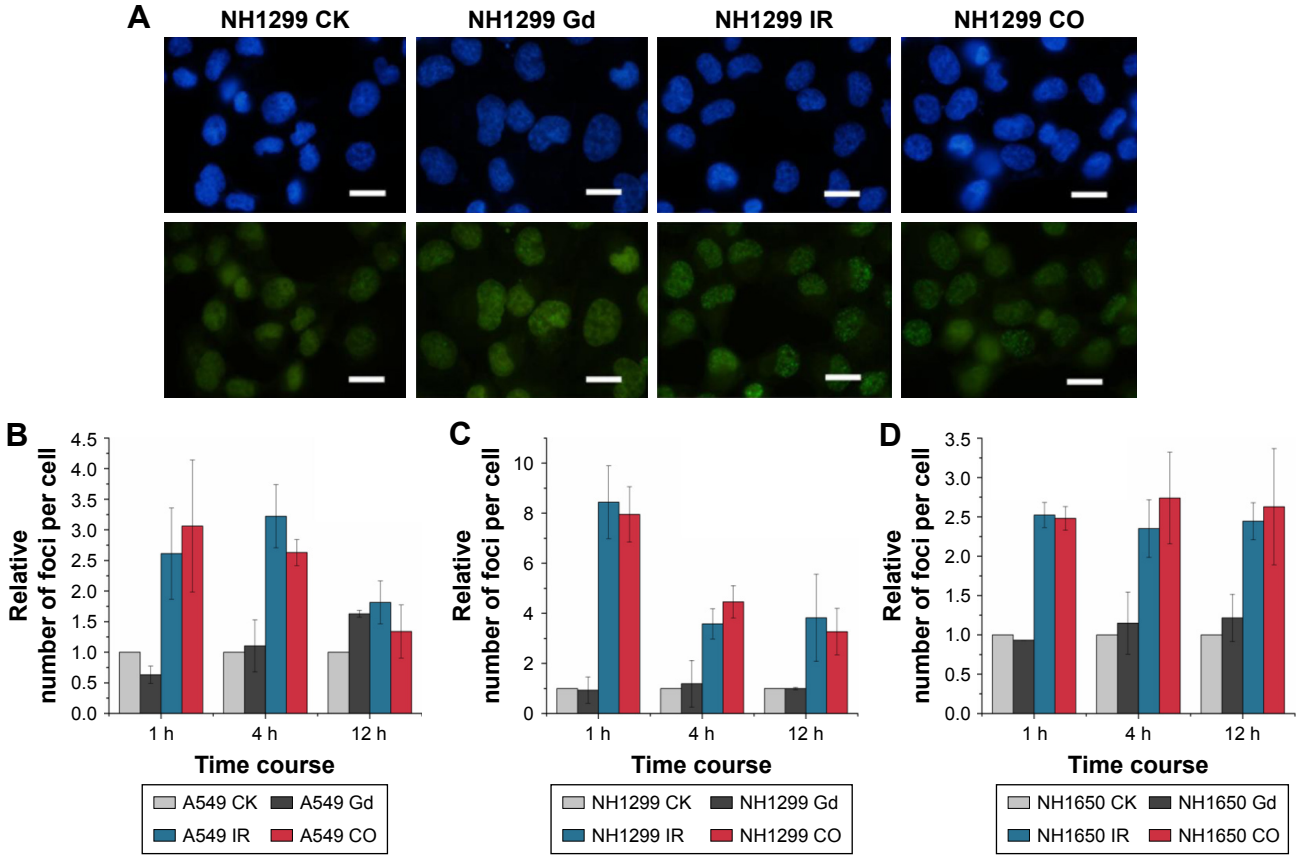

Figure 5 GONs do not increase DNA damage after X-ray irradiation.
Notes: (**A**) DSB images of NH1299 cells at 1 hour post-radiation; scale bar is 20 μm; cell nuclei dyed with Hoechst 33342 are blue; γ-H2AX foci visualized by incubating with indicated fluorescent antibodies are green. Relative foci number per cell in A549 (**B**), NH1299 (**C**), and NH1650 (**D**) cell lines; CO indicates co-treatment with Gd and X-ray irradiation; CK represents the control.
Abbreviations: DSB, double-strand breakages; GONs, gadolinium oxide nanocrystals; Gd, gadolinium; IR, irradiation.

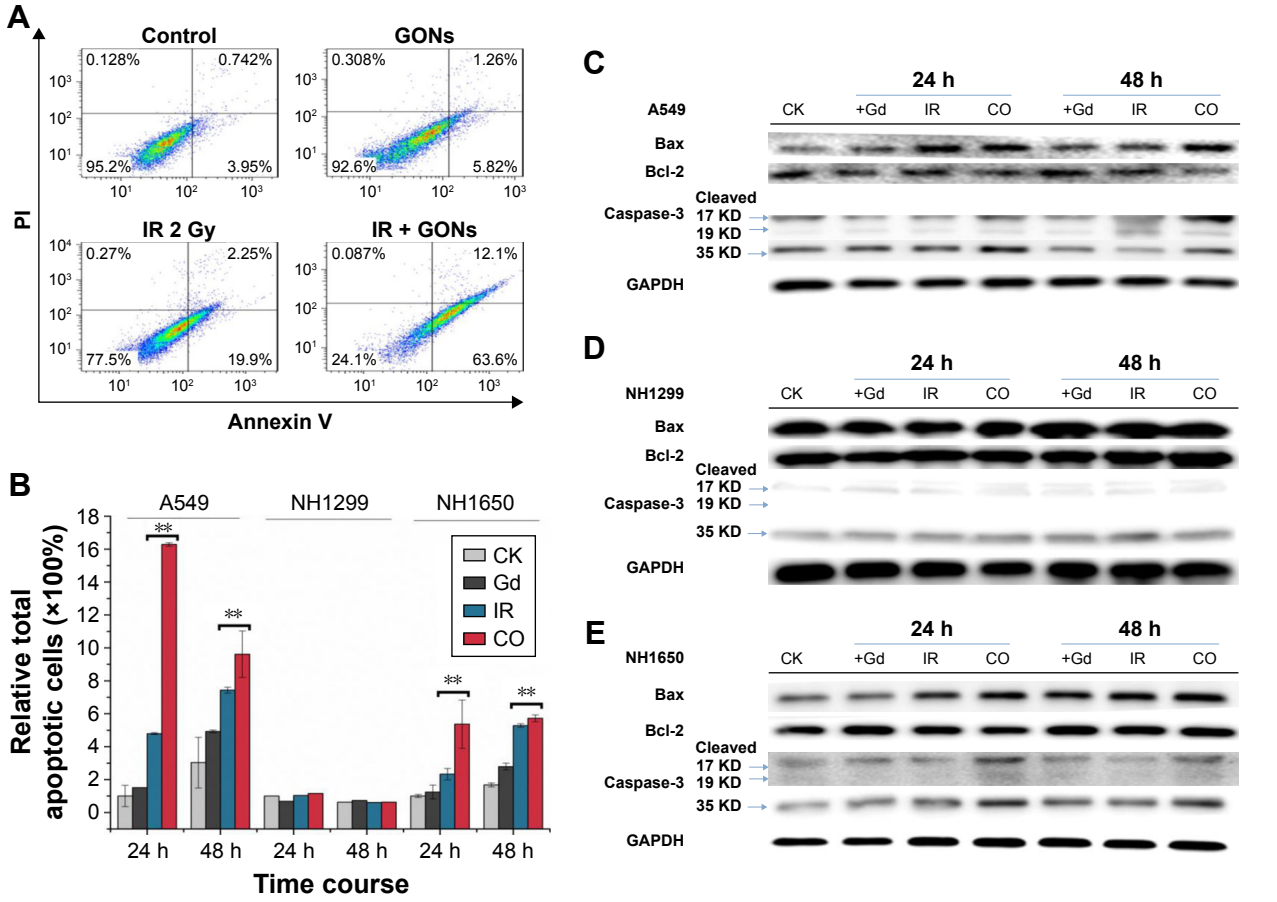

Figure 6 GONs treatment enhances apoptosis in A549 and NH1650 cells but not in NH1299 cells after irradiation.
Notes: (**A**) Apoptotic rates of A549 cells treated with GONs and/or X-ray irradiation at 24 hours posttreatment. (**B**) The relative total apoptotic cell ratio analysis for the three studied cell lines. Western blot analyses of apoptosis-related pivotal proteins in A549 (**C**), NH1299 (**D**), and NH1650 (**E**) cells. CK represents the control; CO represents the co-treatment with irradiation and GONs. $^{**}p<0.01$ represent extremely significant differences.
Abbreviations: GONs, gadolinium oxide nanocrystals; IR, irradiation.

conditions, which is in line with p53 being a key regulator of apoptosis.[33] The Western blot results further verified this point (Figure 6C–E). Co-treatment with X-rays and GONs upregulated the expression of the pro-apoptosis protein Bax and downregulated the expression of the anti-apoptosis protein Bcl-2, leading to cleavage of caspase-3 compared with that of irradiation or GONs treatment alone in A549 and NH1650 cells but not in NH1299 cells. These data indicate that increased apoptosis may be one of the radiosensitizing mechanisms of GONs in A549 and NH1650 cells, but not in NH1299 cells, under X-ray irradiation.

GONs enhance cytostatic autophagy after X-ray irradiation

Whether irradiation-induced autophagy helps to kill cancer cells or to sustain their survival remains controversial.[34,35] We examined the autophagy induced by X-ray irradiation and/or GONs treatment and its influence on radiosensitivity to determine the radiosensitization mechanism of GONs. To quantify the likely induction of autophagy, the presence of acidic vesicular organelles was assayed, which is a characteristic of the autophagy process and can be detected by flow cytometry in combination with acridine orange staining. Flow cytometry images are presented to reflect the autophagy incidence levels in A549, NH1299, and NH1650 cells exposed to X-rays and GONs at 4 hours and 12 hours postirradiation (Figures 7A and S4). Notably, X-ray irradiation treatment alone increased the autophagy rates of the three NSCLC cell lines (Figure 7C–E); furthermore, co-treatment enhanced this trend with a statistically significant difference. In addition, the conjugation of the soluble form of LC3 (LC3-I) with phosphatidylethanolamine and its conversion into a non-soluble form (LC3-II) is a hallmark of autophagy.[36] Consequently, the expression levels of LC3-II in the three studied NSCLC cell lines were measured. At the indicated time points, the LC3-II expression levels induced by combination treatment were more significant than those by radiation treatment alone (Figure 7B).

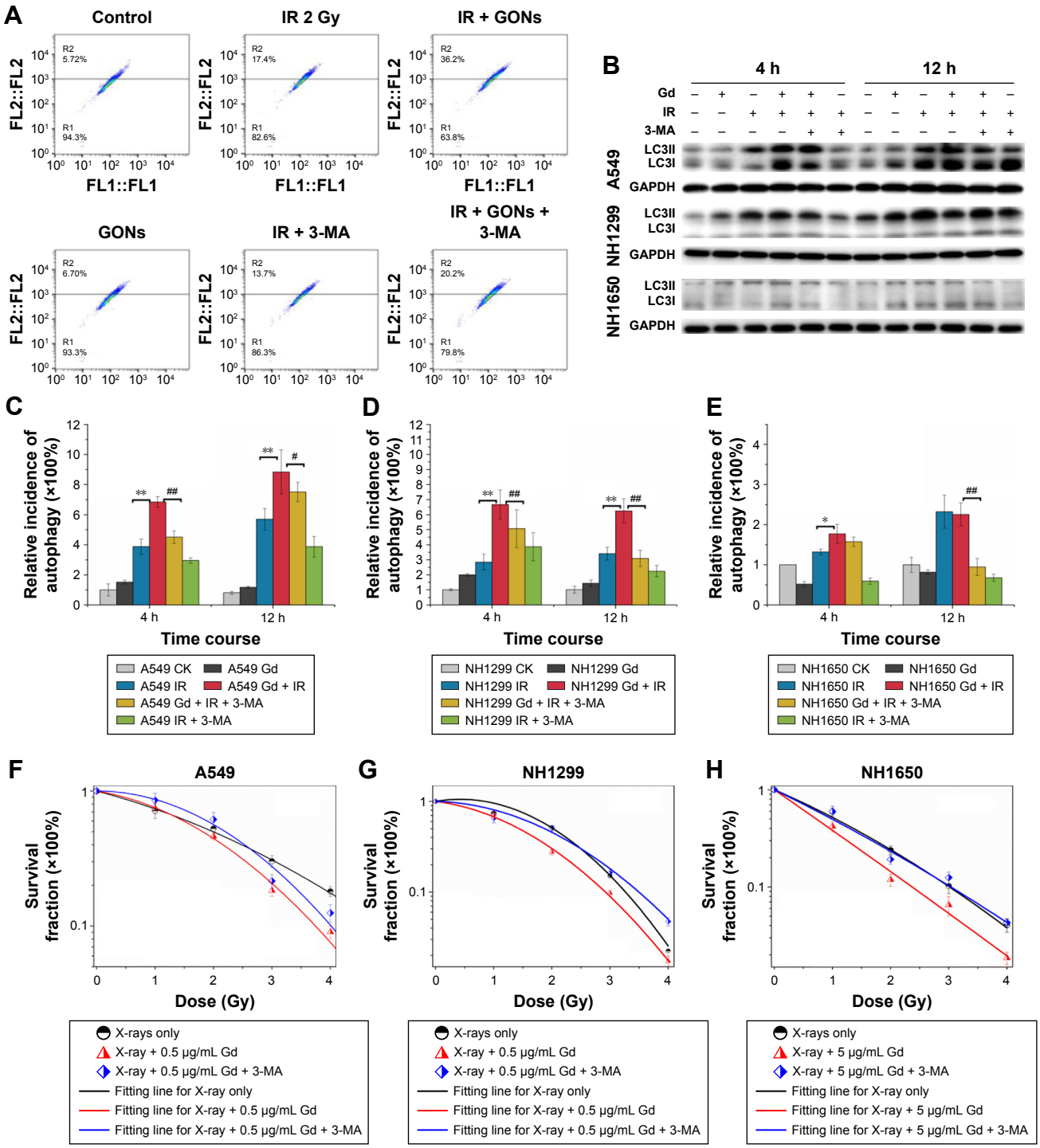

Figure 7 Enhanced cytostatic autophagy caused by GONs under X-ray irradiation.

Notes: (**A**) Autophagy incidence of A549 cells treated with GONs and/or radiation in the absence/presence of 3-MA at 4 hours posttreatment. (**B**) Western blot analysis of the variation in LC3-II toward various treatments for the three cell lines. Autophagic cell ratio analyses detected by flow cytometry for A549 (**C**), NH1299 (**D**), and NH1650 (**E**) cells; $^{*}p<0.05$ and $^{**}p<0.01$ represent statistically significant or extremely significant differences, respectively, between cells irradiated alone and those co-treated with radiation and GONs; $^{\#}p<0.05$ and $^{\#\#}p<0.01$ indicate statistically significant differences in the relative incidence of autophagy by pretreating with 3-MA 4 hours before radiation. (**F**–**H**) Survival fraction of A549 (**F**), NH1299 (**G**), and NH1650 (**H**) cells under combination treatment with radiation and GONs with or without 3-MA; CK represents the control.

Abbreviations: GONs, gadolinium oxide nanocrystals; 3-MA, 3-methyladenine; IR, irradiation; Gd, gadolinium.

To investigate whether autophagy modulates cellular radiosensitivity, a pharmacological inhibitor, 3-MA, which can inhibit autophagic sequestration during the early stage of autophagosome formation,[37] was used. The results from the clonogenic survival study showed that pretreatment with 3-MA improved cell survival compared with that of irradiated groups pretreated with GONs alone (Figure 7F–H). Consistent with these results, in this study, the expression of

LC3-II was reduced after 3-MA co-treatment (Figure 7B). Collectively, these results demonstrate that GONs treatment promotes radiosensitivity through autophagy-induced cell death. To the best of our knowledge, this is the first evidence for the radiosensitizing effect of GONs on NSCLC cells under X-ray irradiation through the promotion of cytostatic autophagy.

Discussion

In this study, we observed an obvious effect in the radiosensitization of NSCLC cells pretreated with GONs in a clonogenic assay. Moreover, the sensitization rate was independent of the Gd concentration in A549 cells. However, a higher Gd concentration (5.0 μg/mL) showed a protective effect in NH1299 cells, which may be due to the hydroxyl radical quenching caused by higher Gd uptake by the cells. In addition to the concentration, the position of Gd within the cells contributed to the radiation enhancement effect. According to a previous study,[19] GONs were dispersed in the cytoplasm but not in the nucleus. Consequently, we hypothesized that nuclear damage, such as DNA damage, was likely not a major cause for the radiosensitization induced by GONs. Our results verified this hypothesis. There was no significant difference in the number of γ-H2AX foci and the distribution of the cell cycle, which are markers of DNA damage, between radiation-alone treatment and GONs co-treatment. Similar results have also been obtained by other researchers.[9,38]

Although radiation-induced nuclear DNA damage, such as single- and double-strand breaks, has been regarded as the main cause of cell death, potential contribution from cytoplasmic damage cannot be ignored. Numerous studies have demonstrated that extranuclear targets may be important in mediating the genotoxic effects of ionizing radiation.[39,40] We have found that mitochondrial dysfunction,[41] endoplasmic reticulum stress (ER stress),[28] and other cytoplasmic damage induced by irradiation lead to apoptosis and autophagy. The presence of Gd in the cytoplasm enhanced this effect, which may be a key factor in radiosensitization. The expression levels of p-Drp1 (a marker of mitochondrial dynamics) and Bip (a marker of ER stress) were upregulated in the co-treatment group compared with those of irradiation-only group (Figure S5). These results confirmed that GONs treatment increased the cytoplasmic damage induced by X-ray irradiation.

Apoptosis is a key mechanism by which ionizing radiation kills tumor cells. The signal that induces apoptosis may come from the nucleus, such as from DNA damage, or from the cytoplasm, such as from mitochondria and/or ER. In A549 and NH1650 cells, we found that their apoptosis rates were upregulated when cells were co-treated with irradiation and GONs; GONs were only present in the cytoplasm and increased the level of damage induced by irradiation. These results indicated that apoptosis enhancement in the cytoplasm was one pathway for the radiosensitization caused by GONs in A549 and NH1650 cells. However, we found similar radiosensitization but not apoptosis upregulation in NH1299 cells. Other pathways may be responsible for the mechanism of GONs-induced radiosensitization in NH1299 cells.

Autophagy is a lysosome-based degradative pathway that plays an essential role in maintaining cellular homeostasis.[42] It has been widely reported that autophagy presents as both a survival mechanism and direct contributor to cell death. Modulating autophagy has recently emerged as a promising therapeutic approach for certain cancer types.[43,44] Nanoparticles have been shown to induce autophagy and have been defined as a novel class of autophagy activators.[45] For example, Ag nanoparticles can induce protective autophagy as a result of ROS upregulation when acting as a radiosensitizer.[46] In addition to the cytoprotective form of autophagy, the cytostatic form of autophagy can be induced to improve the radiation sensitivity of breast cancer cells.[47] In this study, we demonstrated that co-treatment with GONs enhanced autophagy in NH1299 cells; moreover, abrogation of autophagy by the 3-MA inhibitor substantially suppressed cell death. A similar phenomenon was observed in A549 and NH1650 cells. Consequently, cytostatic autophagy played an important role in sensitizing NSCLC cells pretreated with GONs under X-ray irradiation, especially for *p53*-negative NH1299 cells.

Consequently, the presence of GONs led to an increase in hydroxyl radical production and an increase in the generation of ROS in the cytoplasm, contributing to an upregulation of cell oxidative stress, which resulted in increased cytoplasmic damage. Thus, cytostatic autophagy was promoted and, finally, cell death was induced. The radiosensitizing effect of GONs was related to their surface modification and the size of the Gd_2O_3 core. The results observed here can only be used to support the radiosensitizing biomechanism of GONs under X-ray irradiation.

In future work, we will study not only the enhanced cytostatic autophagy induced by other kinds of GONs but also in vivo preclinical studies on their therapeutic efficacy. Since nebulized GdNPs were used as theranostic reagents in lung tumors,[16] the combination of radiotherapy with nanomaterials has been developed as a standard treatment strategy. Currently, immunotherapy has developed into an effective approach for cancer therapy. The combination of

radiotherapy with durvalumab can significantly improve the median progression-free survival of patients with advanced stages of NSCLC.[48] It is hopeful that the progression-free survival and overall survival of patients with NSCLC will be further improved by using immunotherapy following radiotherapy with GdNPs.

Conclusion

In this work, we found that the presence of GONs increased hydroxyl radical production in aqueous solutions and cellular ROS production in vitro. The radiosensitization biomechanism of GONs in tumor cells under X-ray irradiation was both concentration- and cell-dependent. The promotion of autophagic cell death induced by GONs was one of the main biological pathways for radiosensitization in NSCLC cell lines, especially in NH1299 cells which is characteristic by a deletion of p53, namely, specifically in $NH1299^{P53\ (-)}$ cells; moreover, apoptosis and cytostatic autophagy increases contributed to the radiosensitization of GONs in A549 and NH1650 cells. These results present the first evidence for the radiosensitizing effect of GONs on NSCLC cells under X-ray irradiation through the promotion of cytostatic autophagy. Due to their good biocompatibility and great potential for biological tracing, quantitative analytical studies, and early diagnosis of cancers, GONs can be employed as a potential theranostic sensitizer in NSCLC cancer therapy, but further in vivo preclinical studies on their therapeutic efficacy, tumor uptake capacity, and toxicity are needed to define their potential clinical benefits.

Acknowledgments

The authors acknowledge the support from the National Key Research and Development Program (2017YFC0108500), the National Key Technology Support Program of the Ministry of Science and Technology of China (2015BAI01B11), the National Natural Science Foundation of China (11875299), and the CAS Key Laboratory of Heavy Ion Radiation Biology and Medicine, Institute of Modern Physics (2016-01).

Disclosure

The authors report no conflicts of interest in this work.

References

1. Bray F, Ferlay J, Soerjomataram I, Siegel RL, Torre LA, Jemal A. Global Cancer statistics 2018: GLOBOCAN estimates of incidence and mortality worldwide for 36 cancers in 185 countries. *CA Cancer J Clin*. 2018;68(6):394–424.
2. Cao C, D'Amico T, Demmy T, et al. Surgery versus SABR for resectable non-small-cell lung cancer. *Lancet Oncol*. 2015;16(8):e370–e371.
3. Elsayad K, Samhouri L, Scobioala S, Haverkamp U, Eich HT. Is tumor volume reduction during radiotherapy prognostic relevant in patients with stage III non-small cell lung cancer? *J Cancer Res Clin Oncol*. 2018; 144(6):1165–1171.
4. Nieder C, de Ruysscher D, Gaspar LE, et al. Reirradiation of recurrent node-positive non-small cell lung cancer after previous stereotactic radiotherapy for stage I disease. *Strahlenther Onkol*. 2017;193(7): 515–524.
5. Zhu Z-F, Ma HL, Fan M, et al. Sequential chemoradiotherapy with accelerated hypofractionated radiotherapy compared to concurrent chemoradiotherapy with standard radiotherapy for locally advanced non-small cell lung cancer. *Technol Cancer Res Treat*. 2014;13(3): 269–275.
6. Ramroth J, Cutter DJ, Darby SC, et al. Dose and fractionation in radiation therapy of curative intent for non-small cell lung cancer: meta-analysis of randomized trials. *Int J Radiat Oncol Biol Phys*. 2016;96(4):736–747.
7. Kim J, Piao Y, Hyeon T. Multifunctional nanostructured materials for multimodal imaging, and simultaneous imaging and therapy. *Chem Soc Rev*. 2009;38(2):372–390.
8. Ahmad R, Royle G, Lourenço A, Schwarz M, Fracchiolla F, Ricketts K. Investigation into the effects of high-Z nano materials in proton therapy. *Phys Med Biol*. 2016;61(12):4537–4550.
9. Kuncic Z, Lacombe S. Nanoparticle radio-enhancement: principles, progress and application to cancer treatment. *Phys Med Biol*. 2018; 63(2):02TR01.
10. Liu Y, Zhang P, Li F, et al. Metal-based *NanoEnhancers* for Future Radiotherapy: Radiosensitizing and Synergistic Effects on Tumor Cells. *Theranostics*. 2018;8(7):1824–1849.
11. Cui L, Her S, Borst GR, Bristow RG, Jaffray DA, Allen C. Radiosensitization by gold nanoparticles: will they ever make it to the clinic? *Radiother Oncol*. 2017;124(3):344–356.
12. Her S, Jaffray DA, Allen C. Gold nanoparticles for applications in cancer radiotherapy: mechanisms and recent advancements. *Adv Drug Deliv Rev*. 2017;109:84–101.
13. Kotb S, Detappe A, Lux F, et al. Gadolinium-based nanoparticles and radiation therapy for multiple brain melanoma metastases: proof of concept before phase I trial. *Theranostics*. 2016;6(3):418–427.
14. Lux F, Verry C, Dufort S, Tillement O, Le Duc G, Balosso J. Ultrasmall theranostic nanoparticles for the treatment of multiple brain metastases by radiation therapy: a first in man. *Int J Radiat Oncol Biol Phys*. 2017;99(2):Suppl, E34.
15. Le Duc G, Miladi I, Alric C, et al. Toward an image-guided microbeam radiation therapy using gadolinium-based nanoparticles. *ACS Nano*. 2011;5(12):9566–9574.
16. Dufort S, Bianchi A, Henry M, et al. Nebulized gadolinium-based nanoparticles: a theranostic approach for lung tumor imaging and radiosensitization. *Small*. 2015;11(2):215–221.
17. Park JY, Baek MJ, Choi ES, et al. Paramagnetic ultrasmall gadolinium oxide nanoparticles as advanced T1 MRI contrast agent: account for large longitudinal relaxivity, optimal particle diameter, and in vivo T1 MR images. *ACS Nano*. 2009;3(11):3663–3669.
18. Ahrén M, Selegård L, Klasson A, et al. Synthesis and characterization of PEGylated Gd_2O_3 nanoparticles for MRI contrast enhancement. *Langmuir*. 2010;26(8):5753–5762.
19. Ma X-H, Gong A, Xiang LC, et al. Biocompatible composite nanoparticles with large longitudinal relaxivity for targeted imaging and early diagnosis of cancer. *J Mater Chem B*. 2013;1(27):3419–3428.
20. Faucher L, Tremblay M, Lagueux J, Gossuin Y, Fortin MA. Rapid synthesis of PEGylated ultrasmall gadolinium oxide nanoparticles for cell labeling and tracking with MRI. *ACS Appl Mater Interfaces*. 2012; 4(9):4506–4515.
21. Amirrashedi M, Alam NR, Mostaara S, Haghgoo S, Gorji E, Jaberi R. Dose enhancement in radiotherapy by novel application of gadolinium based MRI contrast agent Nanomagnetic particles in gel dosimetry. *Ifmbe Proc*. 2015;51:816–822.

22. Seo SJ, Han SM, Cho JH, et al. Enhanced production of reactive oxygen species by gadolinium oxide nanoparticles under core-inner-shell excitation by proton or monochromatic X-ray irradiation: implication of the contribution from the interatomic de-excitation-mediated nanoradiator effect to dose enhancement. *Radiat Environ Biophys*. 2015; 54(4):423–431.
23. Liu Y, Liu X, Jin X, et al. The dependence of radiation enhancement effect on the concentration of gold nanoparticles exposed to low- and high-LET radiations. *Phys Med*. 2015;31(3):210–218.
24. Liu X, Liu Y, Jin X, et al. Radiosensitizing effect of functionalized gold nanoparticles on human hepatoma HepG2 cells. *Nanomedicine*. 2016;12(2):546.
25. Liu Y, Liu X, Zhang P, et al. The synergistic radiosensitizing effect of tirapazamine-conjugated gold nanoparticles on human hepatoma HepG2 cells under X-ray irradiation. *Int J Nanomed*. 2016;11: 3517–3531.
26. Söderlind F, Pedersen H, Petoral RM, Käll P-O, Uvdal K. Synthesis and characterisation of Gd2O3 nanocrystals functionalised by organic acids. *J Colloid Interface Sci*. 2005;288(1):140–148.
27. Liu Y, Liu X, Jin X, et al. The radiation enhancement of 15 nm Citrate-Capped gold nanoparticles exposed to 70 keV/μm carbon ions. *J Nanosci Nanotechnol*. 2016;16(3):2365–2370.
28. Li F, Zheng X, Liu Y, et al. Different roles of CHOP and JNK in mediating radiation-induced autophagy and apoptosis in breast cancer cells. *Radiat Res*. 2016;185(5):539–548.
29. Wen Y, Zhang W, Gong N, et al. Carrier-free, self-assembled pure drug nanorods composed of 10-hydroxycamptothecin and chlorin e6 for combinatorial chemo-photodynamic antitumor therapy in vivo. *Nanoscale*. 2017;9(38):14347–14356.
30. Aranda A, Sequedo L, Tolosa L, et al. Dichloro-dihydro-fluorescein diacetate (DCFH-DA) assay: a quantitative method for oxidative stress assessment of nanoparticle-treated cells. *Toxicol In Vitro*. 2013; 27(2):954–963.
31. Pouget JP, Mather SJ. General aspects of the cellular response to low- and high-LET radiation. *Eur J Nucl Med*. 2001;28(4):541–561.
32. Vandersickel V, Depuydt J, van Bockstaele B, et al. Early increase of radiation-induced γH2AX foci in a human Ku70/80 knockdown cell line characterized by an enhanced radiosensitivity. *J Radiat Res*. 2010;51(6):633–641.
33. Kriegs M, Can Y, Brammer I, et al. Radiosensitization of NSCLC cells by EGFR inhibition is the result of an enhanced p53-dependent G1 arrest. *Strahlenther Onkol*. 2015;191:S82.
34. Jin X, Liu Y, Ye F, et al. Role of autophagy in high linear energy transfer radiation-induced cytotoxicity to tumor cells. *Cancer Sci*. 2014; 105(7):770–778.
35. Chaachouay H, Ohneseit P, Toulany M, Kehlbach R, Multhoff G, Rodemann HP. Autophagy contributes to resistance of tumor cells to ionizing radiation. *Radiother Oncol*. 2011;99(3):287–292.
36. Klionsky DJ, Abdalla FC, Abeliovich H, et al. Guidelines for the use and interpretation of assays for monitoring autophagy. *Autophagy*. 2012;8(4):445–544.
37. Chen S, Rehman SK, Zhang W, Wen A, Yao L, Zhang J. Autophagy is a therapeutic target in anticancer drug resistance. *Biochim Biophys Acta*. 2010;1806(2):220–229.
38. Stefančíková L, Porcel E, Eustache P, et al. Cell localisation of gadolinium-based nanoparticles and related radiosensitising efficacy in glioblastoma cells. *Cancer Nanotechnol*. 2014;5(1):6.
39. Yasui H, Takeuchi R, Nagane M, et al. Radiosensitization of tumor cells through endoplasmic reticulum stress induced by PEGylated nanogel containing gold nanoparticles. *Cancer Lett*. 2014;347(1):151–158.
40. Sonnenblick BP. Neotetrazolium as a visible indicator of radiation damage – reaction of allium cytoplasm to X-radiation. *Genetics*. 1953; 38(6):692–693.
41. Jin X, Li F, Liu B, et al. Different mitochondrial fragmentation after irradiation with X-rays and carbon ions in HeLa cells and its influence on cellular apoptosis. *Biochem Biophys Res Commun*. 2018;500(4): 958–965.
42. Bhat P, Kriel J, Shubha Priya B, Shubha Priya B, Shivananju NS, Loos B. Modulating autophagy in cancer therapy: advancements and challenges for cancer cell death sensitization. *Biochem Pharmacol*. 2018;147:170–182.
43. Kroemer G, Levine B. Autophagic cell death: the story of a misnomer. *Nat Rev Mol Cell Biol*. 2008;9(12):1004–1010.
44. Apel A, Herr I, Schwarz H, Rodemann HP, Mayer A. Blocked autophagy sensitizes resistant carcinoma cells to radiation therapy. *Cancer Res*. 2008;68(5):1485–1494.
45. Zabirnyk O, Yezhelyev M, Seleverstov O. Nanoparticles as a novel class of autophagy activators. *Autophagy*. 2007;3(3):278–281.
46. Wu H, Lin J, Liu P, et al. Reactive oxygen species acts as executor in radiation enhancement and autophagy inducing by AgNPs. *Biomaterials*. 2016;101:1–9.
47. Gewirtz DA, Hilliker ML, Wilson EN. Promotion of autophagy as a mechanism for radiation sensitization of breast tumor cells. *Radiother Oncol*. 2009;92(3):323–328.
48. Antonia SJ, Villegas A, Daniel D, et al. Durvalumab after chemoradiotherapy in stage III non-small-cell lung cancer. *N Engl J Med*. 2017;377(20):1919–1929.

Supplementary materials

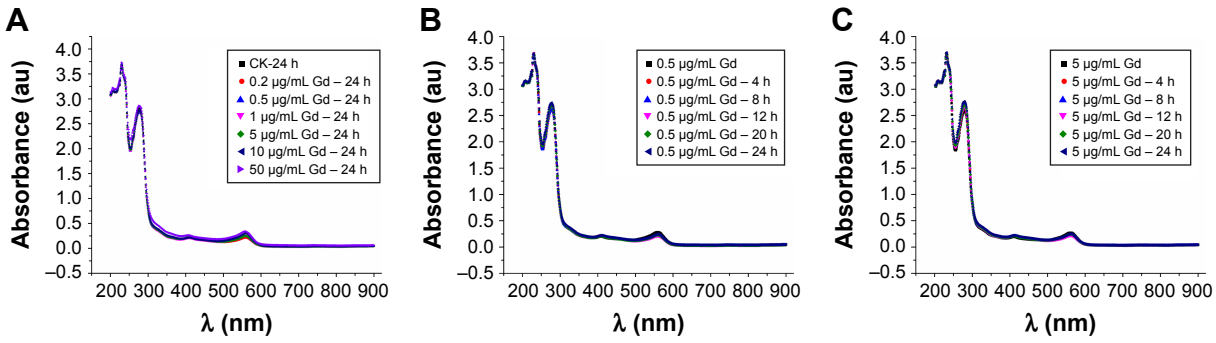

Figure S1 Ultraviolet-visible spectra results confirm that GON solution is very stable in RPMI 1640 medium.
Notes: (**A**) Absorbance of GON with different concentrations after incubating at 37°C for 24 hours. (**B**, **C**) Absorbance of GON at concentrations 0.5 μg/mL (**B**) and 5.0 μg/mL (**C**) at various incubation time.
Abbreviation: GONs, gadolinium oxide nanocrystals.

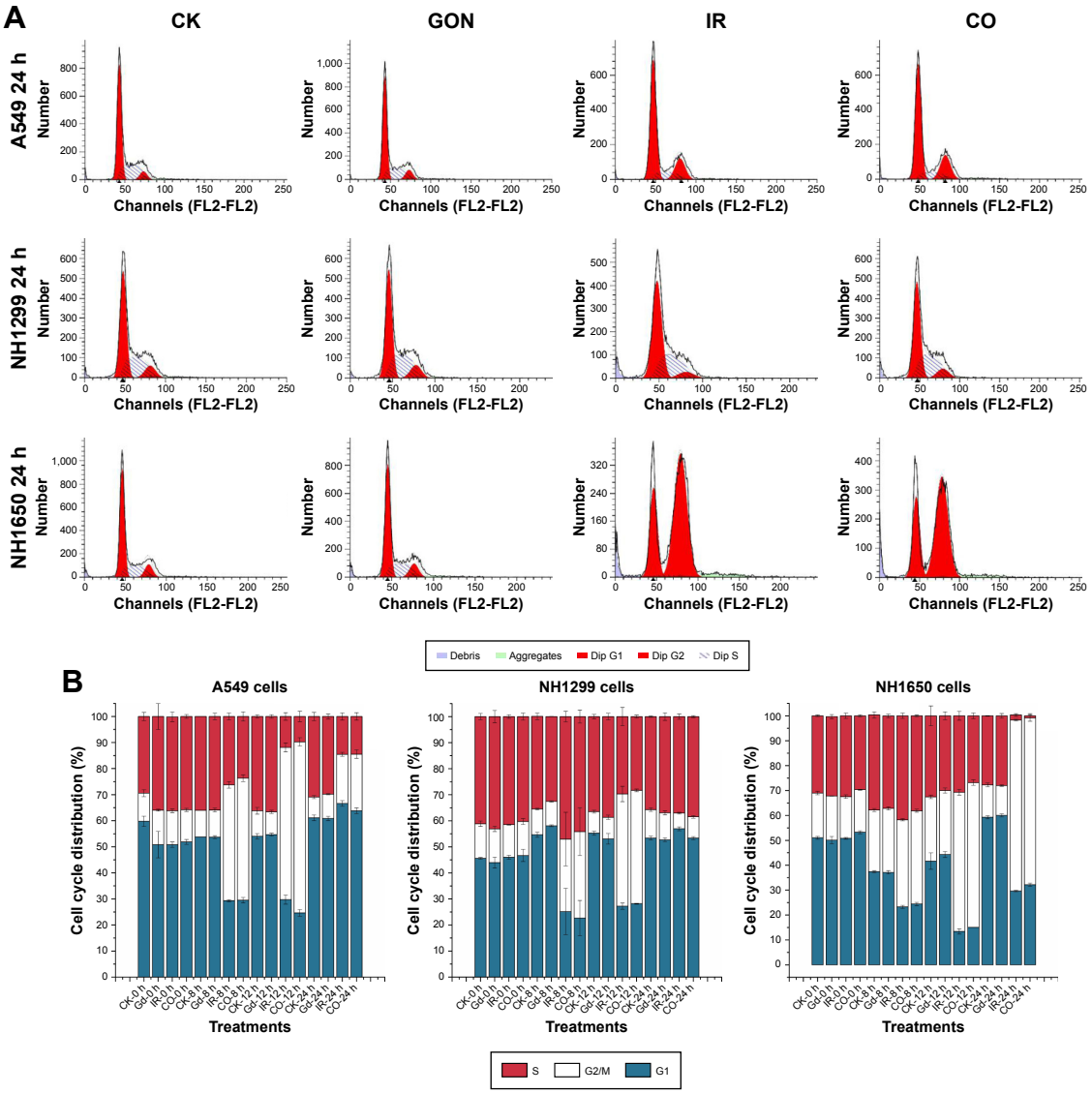

Figure S2 The influence of GON on cell cycle distribution.
Notes: (**A**) Cell flow spectra at 24 hours after X-ray irradiation. (**B**) Cell cycle distributions of three studied cells on time. CK represents the control; CO represents co-treatment with irradiation and GONs.
Abbreviations: GONs, gadolinium oxide nanocrystals; Gd, gadolinium; IR, irradiation.

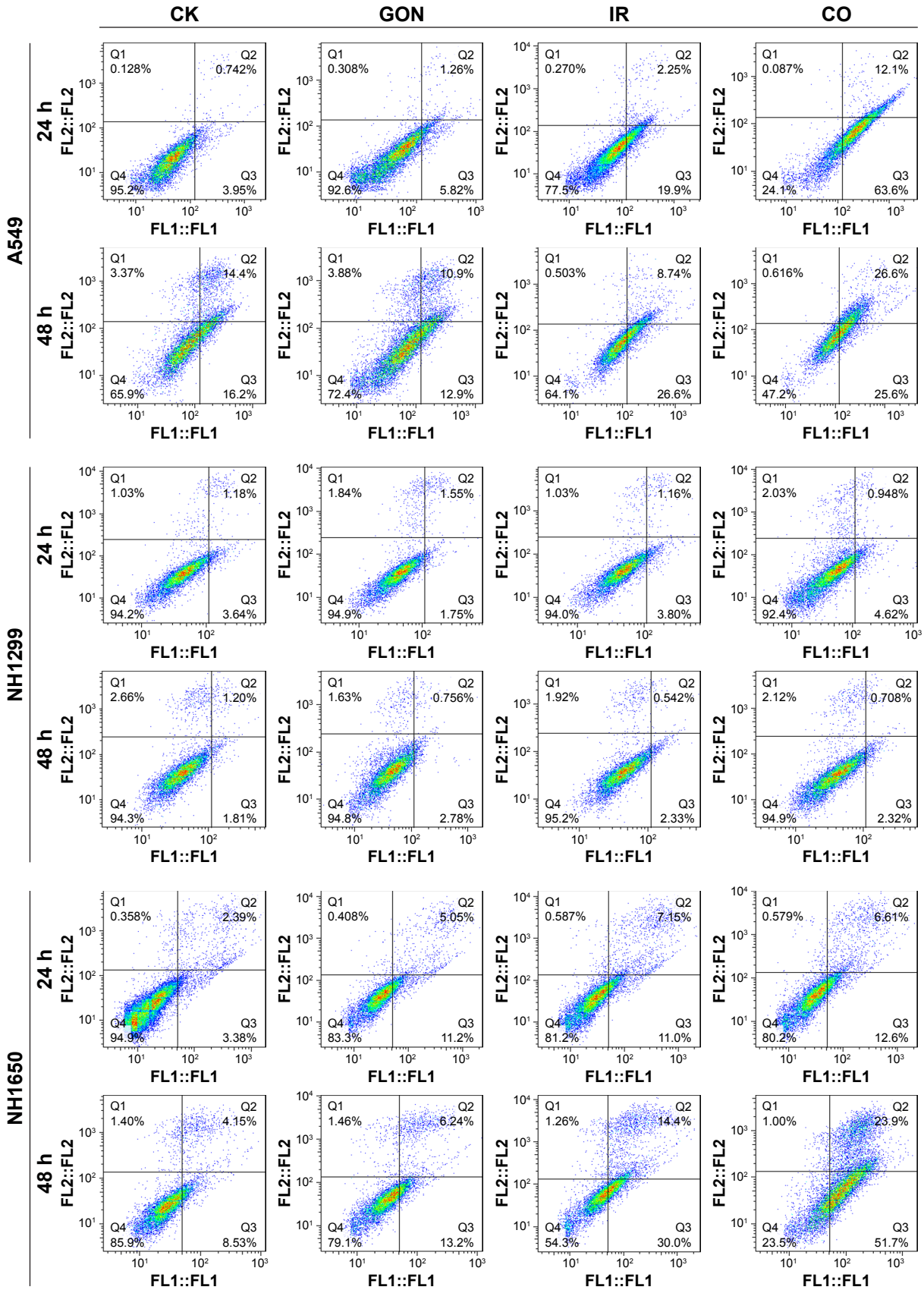

Figure S3 Apoptotic rates of A549, NH1299, and NH1650 cells treated with GON and/or radiation for 24-hour and 48-hour posttreatment.
Note: CK represents the control; CO represents co-treatment with irradiation and GONs.
Abbreviations: GONs, gadolinium oxide nanocrystals; Gd, gadolinium; IR, irradiation.

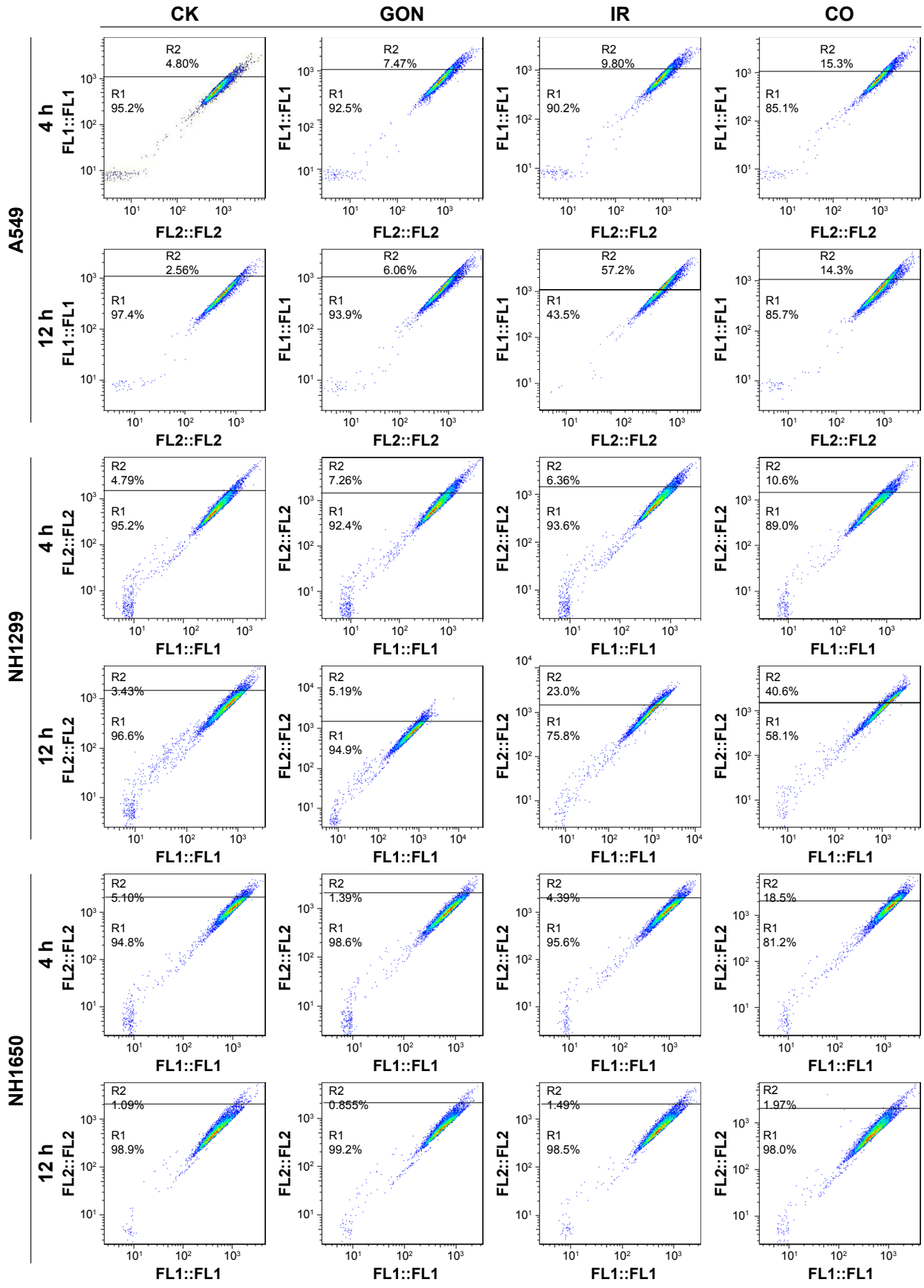

Figure S4 Autophagy incidence of A549, NH1299, and NH1650 cells treated with GON and/or X-ray irradiation for 4-hour and 12-hour posttreatment.
Note: CK represents the control; CO represents co-treatment with irradiation and GONs.
Abbreviations: GONs, gadolinium oxide nanocrystals; Gd, gadolinium; IR, irradiation.

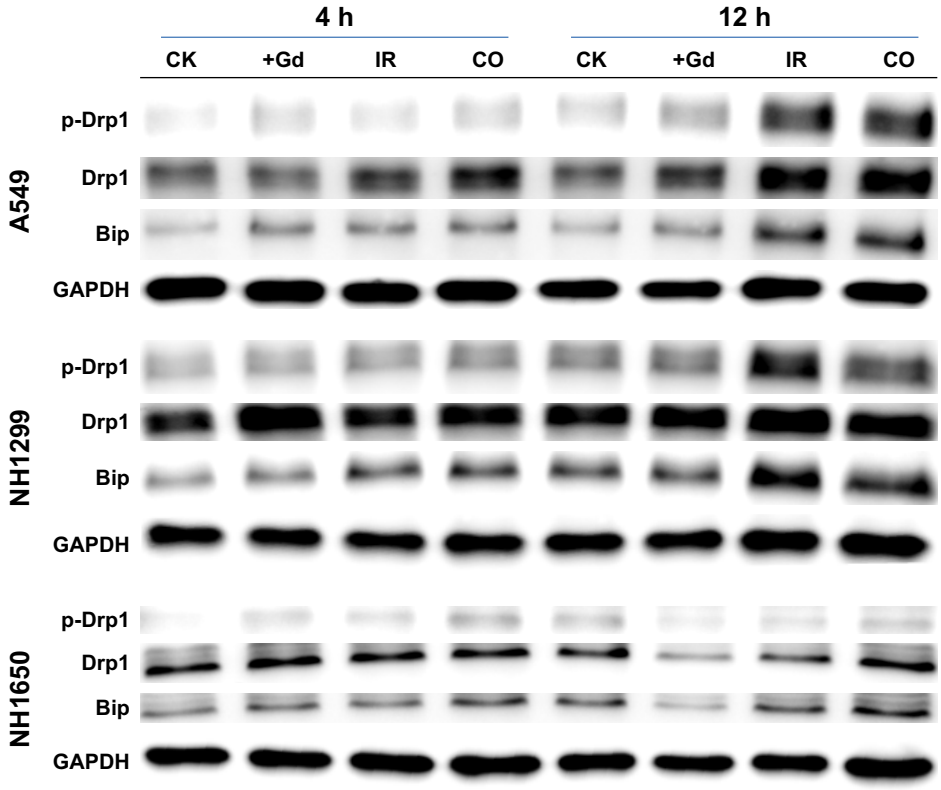

Figure S5 Radiation-induced damages in cytoplasm stimulate the ER stress and mitochondrion dysfunction.
Note: CK represents the control; CO represents co-treatment with irradiation and GONs.
Abbreviations: ER, endoplasmic reticulum; Gd, gadolinium; IR, irradiation.